Article

pubs.acs.org/Biomac

Synthesis of Polyglutamide-Based Metal-Chelating Polymers and Their Site-Specific Conjugation to Trastuzumab for Auger Electron Radioimmunotherapy

Yijie Lu,[†,⊥] Ghislaine Ngo Ndjock Mbong,[‡,⊥] Peng Liu,[†] Conrad Chan,[‡] Zhongli Cai,[‡] Dirk Weinrich,[†] Amanda J. Boyle,[‡] Raymond M. Reilly,*[,‡,§,∥] and Mitchell A. Winnik*[,†]

[†]Department of Chemistry, University of Toronto, 80 St. George Street, Toronto, Ontario M5S 3H6, Canada

[‡]Department of Pharmaceutical Sciences, University of Toronto, 144 College Street, Toronto, Ontario M5S 3M2, Canada

[§]Department of Medical Imaging, University of Toronto, 263 McCaul Street, Toronto, Ontario M5T 1W7, Canada

[∥]Toronto General Research Institute, University Health Network, Toronto, Ontario M5G 2M9, Canada

Supporting Information

ABSTRACT: Three types of metal-chelating polymers (MCPs) with hydrazide end groups were synthesized. (1) The first set of polymers (the F-series) was synthesized with a furan end group, and all of the pendant groups along the chain carried only a diethylenetriaminepentaacetic acid (DTPA) metal-chelating functionality. The hydrazide was introduced via a Diels–Alder reaction between the furan and 3,3′-*N*-[ε-maleimidocaproic acid] hydrazide (EMCH). (2) The P-series polymers was designed to carry several copies of a nuclear-localization peptide sequence (NLS peptides, CGYGPKKKRKVGG, harboring the NLS from the simian virus 40 large T-antigen) in addition to the DTPA metal-chelating groups. (3) The third type of polymer (the P-Py series) was a variation of the P-series polymers but with the introduction of a small number of pyrene chromophores along the backbone to allow for UV measurement of the incorporation of the MCPs into trastuzumab (tmab). These hydrazide-terminated polymers were site-specifically conjugated to aldehyde groups generated by $NaIO_4$ oxidation of the pendant glycan in the Fc domain of tmab. The immunoconjugates were radiolabeled with ^{111}In and analyzed by SE–HPLC to confirm the attachment of the polymer to the antibody. HER2 binding assays demonstrated that neither the MCPs nor the presence of the NLS peptides interfered with specific antigen recognition on SK-Br-3 cells, although nonspecific binding was increased by polymer conjugation. Our results suggest that MCPs can be site-specifically attached to antibodies via oxidized glycans in the Fc domain and labeled with ^{111}In to construct radioimmunoconjugates with preserved immunoreactivity.

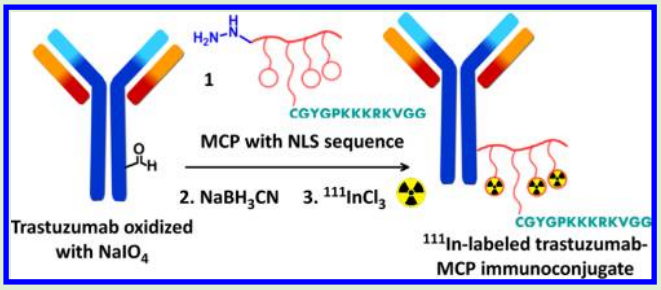

INTRODUCTION

Human epidermal growth factor receptor-2 (HER2) is overexpressed in 20–25% of cases of breast cancer and is the target of the immunotherapeutic agent, trastuzumab (Herceptin).[1−3] Although trastuzumab (tmab) is effective for treatment of highly HER2-amplified breast cancer,[4] there is a need for more potent forms of the drug that are effective against HER2-positive tumors that are resistant to it because of they have lower HER2 density or because they have acquired resistance through other mechanisms.[5] One approach couples HER2 targeting using tmab with the delivery of cytotoxic agents to tumor cells.[4−11] Another approach of particular interest to us is to generate radioimmunoconjugates (RICs) by labeling tmab with cytotoxic radionuclides. Initial experiments involved Auger electron radioimmunotherapy with tmab derivatized with diethylenetriaminepentaacetic acid (DTPA) for labeling with ^{111}In.[12−15] Auger electrons are very low-energy (<25 keV) electrons that have high linear energy transfer because of their nanometer to micrometer range, but Auger electrons cause lethal DNA double-strand breaks only if the decay occurs in close proximity to the cell nucleus. Thus, we also modified the tmab–DTPA immunoconjugates with a nuclear-localization peptide sequence (NLS). Although the ^{111}In–NLS–tmab (specific activity, 240 MBq/mg; 3.6×10^{10} MBq/mol) was 6-fold more potent, on a concentration basis, at decreasing the clonogenic survival of HER2-amplified SK-Br-3 cells with high HER2 density ($1–2 \times 10^6$ per cell) than that of unlabeled tmab, the effectiveness of this approach is limited by the fact that only about 1 in 50 antibodies were labeled with ^{111}In at this specific activity.[4]

To increase the amount of ^{111}In delivered per HER2 recognition event, we explored the idea of using metal-chelating

Received: February 3, 2014
Revised: April 3, 2014
Published: May 16, 2014

polymers (MCPs) carrying many DTPA groups along the backbone as a strategy for increasing the specific activity of the RICs.[16−19] To simplify construction of the RIC and to enable us to screen a family of different polymers with different backbones and different chain lengths, we synthesized a series of polymers, each with a biotin end group. In parallel, we derivatized the Fab fragment of tmab (tmFab) with streptavidin (SAv) using a poly(ethylene glycol) (PEG) spacer with 24 ethylene glycol units. In this way, we were able to take advantage of the strong and rapid binding between biotin and SAv to construct a family of RICs. By surface plasmon resonance experiments, we showed that, for one family of polymers, attachment of the MCP to the tmFab−SAv conjugates had no significant effect on the rate of binding to the extracellular domain of HER2 or the dissociation rate and that the interaction was characterized by a low nanomolar binding constant.[20] Biodistribution studies in Balb/C mice showed that the tissue distribution of these tmFab−SAv−MCP complexes was sensitive both to the chemical structure of the polymer backbone (polyacrylamide, polyaspartamide, or polyglutamide) as well as to the nature of the pendant group to which the DTPA units were attached.[17] We also found that the maximum specific activity of these complexes increased linearly with the number of DTPA units per polymer chain.[16]

Although these survey experiments are useful for demonstrating HER2 recognition of these complexes and for assessing aspects of how polymer structure and chain length affect the properties of the RICs, these complexes are not suitable for therapeutic applications. The main problem is the use of SAv for assembling the complexes: SAv is immunogenic and it also promotes uptake by the kidneys.[21] For therapeutic applications, we need to develop chemistry for direct covalent attachment of the MCP to the antibody. One approach that we have reported in the past is to react MCPs carrying a maleimide end group with thiols obtained by selective reduction of disulfide bonds in the hinge region of an antibody. This type of attachment of MCPs to monoclonal antibodies was developed to construct reagents for mass cytometry.[22−24] Here, we take a different approach. We target our polymers to the glycan attached to the Fc domain of tmab. In this way, polymer attachment will have a minimal influence on the antigen recognition of the RIC.

In our biodistribution studies of biotin end-capped MCPs and their complexes with tmFab−SAv in Balb/C mice,[17] we examined some polymers with a diethylenetriamine (DET) spacer between the polymer backbone and the DTPA metal-chelating group. This spacer has the advantage that at neutral pH the net negative charge of the -DTPA^{4-}/In^{3+} complex is balanced by the positive charge associated with the protonated secondary amine of the DET.[17,18] Tissue distribution studies in Balb/C mice showed a strong propensity for liver uptake of MCPs with multiple negative charges along the backbone. Here, we focus on in vitro experiments, examining tmab−MCP interactions with SK-Br-3 cells where this is not an issue. Because subsequent pendant group transformations are less complicated for PGlu(EDA) than for PGlu(DET), we focus here on tmab−MCP constructs with ethylene diamine (EDA) spacers for pendant group attachment. To proceed, we designed MCPs based on a polyglutamide backbone with a hydrazide end group. At the same time, we optimized conditions for periodate oxidation of the tmab−glycan to generate aldehyde groups. In a later section of this article, we show that these MCPs can be covalently linked to the antibody through hydrazone formation in the presence of $NaBH_3CN$. We faced several challenges in developing the synthesis. The first was end group control coupled with introducing the pendant DTPA groups. The second was controlling the degree of pendant group modification to permit the introduction of fluorescent dyes or sites for attachment of NLS peptides. MCPs with NLS peptide pendant groups will allow us to test another hypothesis in future experiments, namely, that these peptides will promote or enhance nuclear localization of the tmab−MCP RICs.

EXPERIMENTAL SECTION

Materials and Methods. All reagents and solvents were used without further purification unless otherwise noted. Water was purified through a Milli-Q water purification system (18 MΩ cm). All buffers were prepared in our laboratory. Spectra/Pro dialysis membranes (MWCO 1 kDa) were purchased from Spectrum Laboratories, Inc. Millipore Amicon spin filters (15 mL, 3 kDa MWCO; 0.5 mL, 30 kDa MWCO) were purchased from Fisher Scientific, Canada. $^{111}InCl_3$ was purchased from Nordion (Kanata, ON, Canada). 4-(4,6-Dimethoxy-1,3,5-triazin-2-yl)-4-methylmorpholinium chloride (DMTMM, Acros Organics, 99+%) was from Fisher Scientific, Canada. L-Glutamic acid γ-benzyl ester (BLG), *N*,*N*-dimethylformamide (DMF) anhydrous, *N*-methylpyrrolidone (NMP), dichloridemethane (DCM) anhydrous, ethylene diamine (EDA), adipic acid dihydrazide, 2,2-dimethyl-1,3-dioxolane-4-methanamine, furfurylamine, and sodium periodate were purchased from Sigma-Aldrich. 3,3′-*N*-[ε-Maleimidocaproic acid] hydrazide, trifluoroacetic acid salt (EMCH) was purchased from Pierce, Thermo Fisher Scientific Inc. 2-(4-Aminobenzyl)-diethylene-triaminepentaacetic acid (*p*-NH_2-Bn-DTPA) was purchased from Macrocyclics, Dallas, TX, USA. NLS peptide CGYGPKKKRKVGG was purchased from Biobasic Inc., Markham, ON, Canada. Trastuzumab (Hoffman-La Roche, Mississauga, ON, Canada) was obtained from the Pharmacy Department at the University Health Network. The trastuzumab−(*p*-NH_2-Bn-DTPA) immunoconjugate (tmab−NH-Bn-DTPA) was synthesized as described by Rodwell et al.[25] The synthesis of γ-benzyl-L-glutamate *N*-carboxyanhydride (BLG-NCA) was reported elsewhere.[26]

Polymer Synthesis and Pendant Group Transformations. Experimental details for the syntheses of citraconimido-hexanoic acid (CCHA) and all polymers are presented in the Supporting Information. Representative ^1H NMR spectra of these compounds are presented in Figures S1−S14 of the Supporting Information. Polymer synthesis began with ring-opening polymerization of BLG-NCA initiated by either furfurylamine or 2,2-dimethyl-1,3-dioxolane-4-methanamine. Through a series of postpolymerization modifications, three series of metal-chelating polymers with a hydrazide end were synthesized. The details of these syntheses and characterization are given in the Supporting Information.

Biological Experiments. *Breast Cancer Cells.* SK-Br-3 human breast cancer (BC) cells were obtained from the American Type Culture Collection (ATCC, Manassas, VA, USA). The breast cancer cells were grown at 37 °C in an atmosphere of 5% CO_2. They were cultured in RPMI-1640 medium (Sigma-Aldrich, St. Louis, MO, USA) supplemented with 10% fetal bovine serum. SK-Br-3 human BC cells overexpress the human epidermal growth factor receptor 2 (HER2). The HER2 density of SK-Br-3 is 1.3×10^6 receptors/cell.[12]

Site-Specific Conjugation of Hydrazide−Polyglutamide MCPs to Trastuzumab. tmab−MCP immunoconjugates were constructed after sodium metaperiodate, $NaIO_4$, oxidation of the carbohydrates on the Fc domain of tmab. Hydrazide-end metal-chelating polymers (**F4**, **P6**, or **P7Py**) were used in this study. tmab−NH-Bn-DTPA was synthesized following a protocol described in ref 25 for conjugating 4-aminobenzyl-DTPA to proteins.

Oxidation of Trastuzumab. Trastuzumab (1 mg) in phosphate buffer (100 μL containing 150 mM sodium chloride/10 mM sodium phosphate pH 6.0) was incubated in the dark at room temperature with $NaIO_4$ at a molar ratio ($NaIO_4$/tmab) of 200:1 for 30 min. Oxidized tmab containing reactive aldehydes was purified with sodium acetate (pH 6.0, 1.0 M) using an Amicon 30 kDa MWCO spin filter to

Scheme 1. Synthesis Route for a Hydrazide End-Functional MCP (F4) from a Polymer (F3) with a Furan Terminus

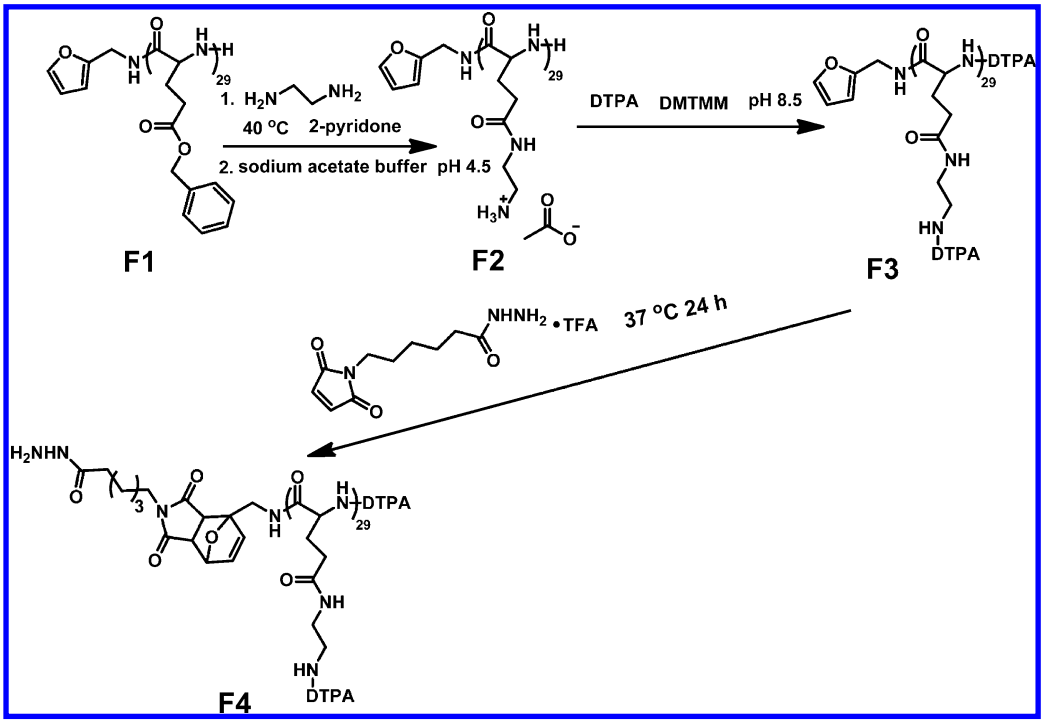

remove the excess of $NaIO_4$. The antibody concentration was measured at 280 nm (1.4 OD_{280} = 1 mg/mL) by a UV−vis spectrometer.

The number of aldehydes generated per molecule of trastuzumab was measured using the colorimetric Purpald (4-amino-3-hydrazino-5-mercapto-1,2,4-triazole) assay, as described by Quesenberry and Lee.[27] Six different standard concentrations of formaldehyde solutions (10−200 μM) were prepared in duplicate in sodium acetate (pH 6.0, 1 M). The absorbance of each standard concentration was measured at 550 nm. The number of aldehydes per tmab was then estimated by dividing the concentration of aldehyde in the solution determined by reference to the standard curve by the tmab concentration.

Reaction of Oxidized Trastuzumab with Hydrazide Polymers. Oxidized tmab was then incubated with a 2-fold molar excess of hydrazide (hy-) metal-chelating polymer (**F4**, **P6**, or **P7Py** at 4 mg/mL) in sodium acetate buffer (1.0 M, pH 6.0, 200 μL) at 25 °C for 2 h. Sodium cyanoborohydride was added to a final concentration of 0.4 mM at 25 °C to reduce the hydrazone linkage formed between the aldehydes and the hydrazide group of the polymer. Unconjugated polymer was removed by a spin filter (0.5 mL 50 kDa MWCO), and the final purity was assessed by size-exclusion high-performance liquid chromatography (SE−HPLC) on a BioSep SEC-4000 column (Phenomenex, Torrance, CA, USA) eluted with 100 mM sodium phosphate buffer (pH 7.0) at a flow rate of 0.35 mL/min that was monitored in line with a diode array detector (PerkinElmer) monitoring at 280 nm and a flow scintillation analyzer (FSA; PerkinElmer) radioactivity detector.

Radiolabeling with ^{111}In of the Trastuzumab−Polymer Immunoconjugates. tmab−hy−MCP conjugates (50−100 μg) were radiolabeled with ^{111}In-acetate (3.7 MBq) for 1 h at room temperature. ^{111}In-acetate was prepared by mixing $^{111}InCl_3$ with 1.0 M sodium acetate buffer, pH 6.0. Labeling efficiency and radiochemical purity were measured by instant thin-layer silica gel chromatography (ITLC−SG; Pall Life Sciences, Ann Arbor, MI, USA) in sodium citrate buffer (pH 5.0, 0.1 M). The retardation factor (R_f) values of ^{111}In-labeled immunoconjugates and free ^{111}In in this system are 0.0 and 1.0, respectively, which shows that the RICs have no mobility on the ITLC−SG plate.

HER2 Immunoreactivity. *One-Point Competition Binding Assay.* The binding of ^{111}In−tmab−hy−MCP (**F4**) to HER2 on SK-Br-3 cells was determined by incubating the RICs (50 μL in phosphate buffered saline, PBS, pH 7.5) with 1 × 10^6 SK-Br-3 cells (100 μL in PBS, pH 7.5) in Eppendorf microtubes (1.5 mL) at 4 °C for 3 h with agitation. The final concentration of RIC was 30 nM. The assays were performed in the absence (total binding) or presence (nonspecific binding) of a 200-fold molar excess of unlabeled tmab. After incubation, the cells were washed twice with PBS, pH 7.5, to remove any unbound radioactivity (supernatant) from the total cellular-bound radioactivity (cell pellets). Cell pellets were collected, and the radioactivity was measured in an automatic γ-counter (Wallac Wizard-1480; PerkinElmer). The percentage of specific binding was calculated by subtracting the percentage of nonspecific binding from the total binding. The percentage of specific binding for ^{111}In−tmab−hy−MCP (**F4**) was compared to ^{111}In-labeled trastuzumab (^{111}In−NH-Bn-DTPA−tmab) derivatized with two *p*-NH_2-Bn-DTPA groups by the same Fc-directed method.[25]

Competition−Binding Assays. Increasing concentrations of the immunoconjugates tmab−hy−MCP (**F4**) or tmab−hy−MCP−NLS (**P6**) (0−2600 nM in 50 μL PBS, pH 7.5) were mixed and incubated with ^{111}In−NH-Bn-DTPA−tmab (20 nM in 50 μL PBS, pH 7.5) in Eppendorf tubes (1.5 mL) containing approximately 1 × 10^6 SK-Br-3 cells (100 μL in PBS, pH 7.5) at 4 °C for 3 h. The cells were then rinsed twice with PBS, pH 7.5, and centrifuged (5 min) initially at 3000*g* and then at 2000*g*. Upon removal of the supernatant (unbound radioactivity), the radioactivity in each cell pellet was measured in a γ-counter. The proportion of ^{111}In-labeled tmab displaced from SK-Br-3 cells by increasing concentrations of tmab−hy−MCP (**F4**) and tmab−hy−MCP−NLS (**P6**) was plotted and fitted to a one-site competition binding model using Prism, ver. 5.0, software (GraphPad, San Diego, CA) to determine the effective concentration for displacement of 50% of the binding (EC_{50}) as well as the dissociation constant (K_D) of the immunoconjugates. HER2-receptor affinity (K_D = 3.2 ± 1.2 nM, see Figure S18) of ^{111}In−NH-Bn-DTPA−tmab was determined in SK-Br-3 cells using methods previously described.[28]

Statistical Analysis. Data are presented as the mean ± standard deviation (SD). Standard errors were calculated using standard error propagation expressions, assuming an uncertainty of ±5% in NMR integrations. Statistical analyses were performed using Prism, ver. 5.0, software. Statistical comparisons were made using Student's *t* test, with $p < 0.05$ indicating statistical significance.

Scheme 2. Synthesis Route for a Hydrazide End-Functional MCP (P6) Harboring NLS Peptides

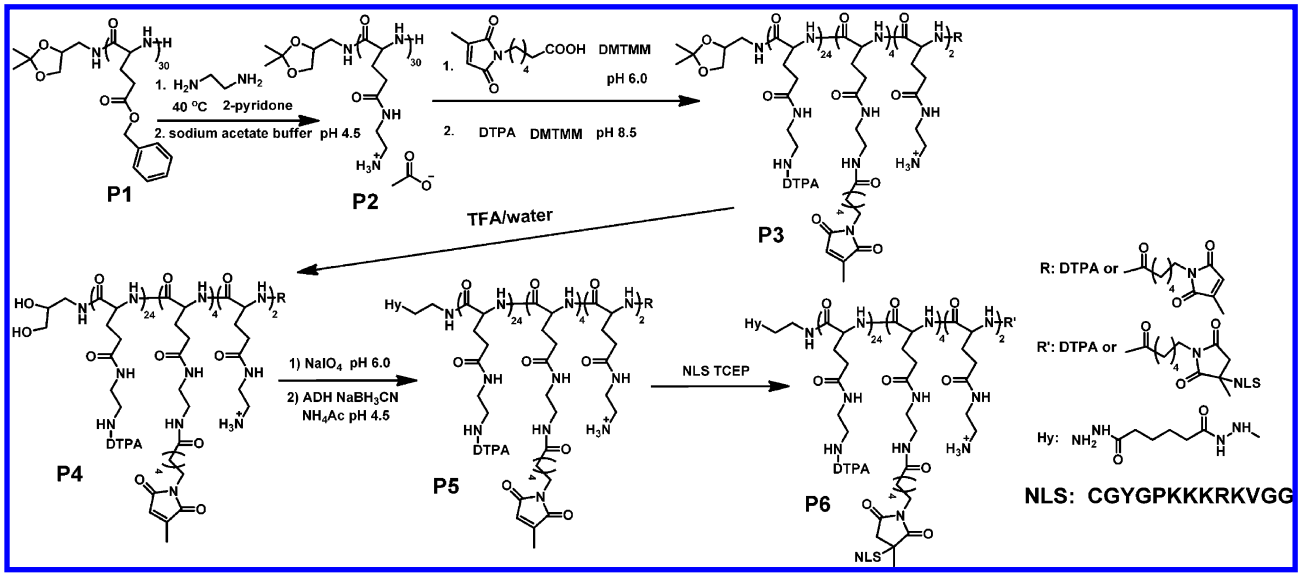

Scheme 3. Synthesis Route for Pyrene-Labeled Hydrazide End-Functional MCP (P7Py) Harboring NLS Peptides

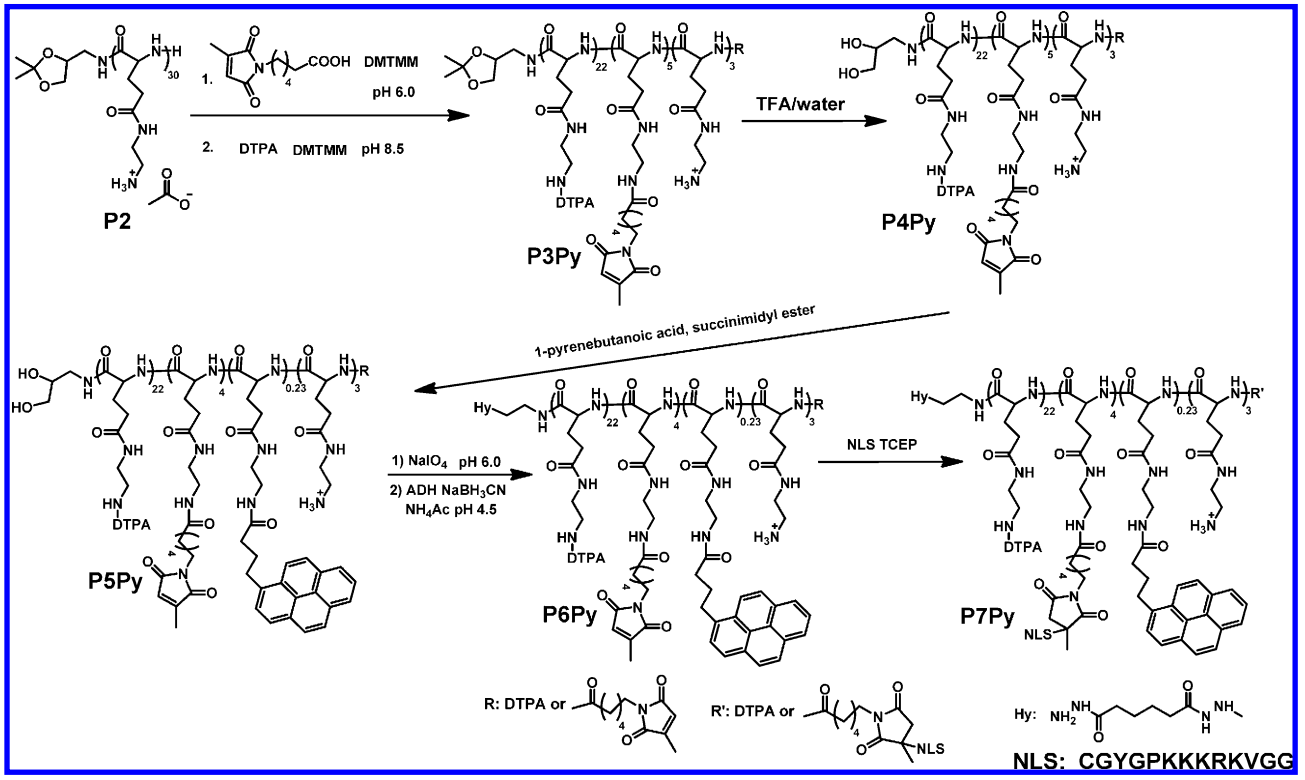

RESULTS AND DISCUSSION

Our philosophy for the synthesis of RICs is based on the idea of site-specific attachment of MCPs with a hydrazide end functionality to aldehyde groups generated by $NaIO_4$ oxidation of the pendant glycans in the Fc domain of tmab. Although end group control was one of the goals for the polymer synthesis, a more difficult challenge was to introduce multiple pendant groups along the polymer backbone. We approached this challenge in stages. Three types of MCPs with hydrazide end groups were synthesized: (1) The first set of polymers (the F-series) was synthesized with a furan end group, and all of the pendant groups along the chain carried only a DTPA metal-chelating functionality. In the final step of the synthesis, the hydrazide was introduced via a Diels–Alder reaction between the furan and EMCH (Scheme 1). (2) The P-series polymers were designed to carry several copies of an NLS peptide in addition to the DTPA metal-chelating groups. This required a synthesis design with a careful balance of orthogonal reactivities so that the NLS peptide could be introduced in a way that did not interfere with the chain end (Scheme 2). (3) The third type of polymer (the P-Py series of MCPs) was a variation of the P-series polymers but with the introduction of a small number of pyrene chromophores along the backbone to allow for UV detection of the MCP (Scheme 3).

dx.doi.org/10.1021/bm500174p | Biomacromolecules 2014, 15, 2027−2037

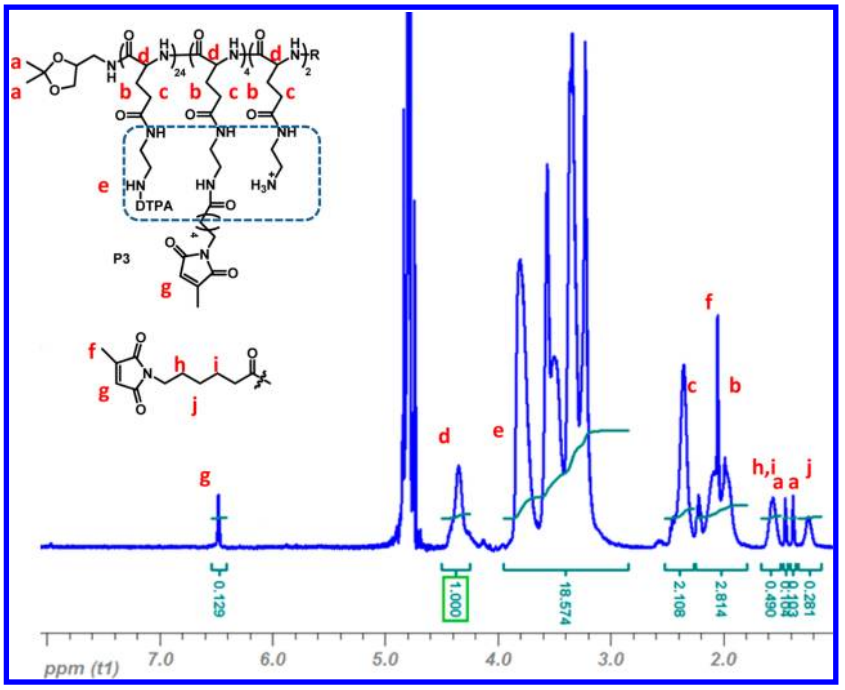

Figure 1. ^{1}H NMR spectrum of polyglutamide with DTPA and citraconimide modified on the pendant group (**P3**). End group analysis shows the degree of polymerization to be 29 by comparing the integration of the acetonide-diol end group signals, a, to that of the backbone methine signal, d. The DTPA functionality was calculated by the integral peak of e (resulting from DTPA and EDA) to the integral of peak d (resulting from the backbone methine). The citraconimide functionality was calculated by the integral of the citraconimide signals, g, to that of the backbone methine, d. Thus, the polymer has, on average, 24 DTPA groups, four citraconimide groups, and two unreacted amino groups. As shown in Scheme 2, the polymer end groups, R, are a mixture of DTPA and MMal groups.

Polymer Synthesis and Chain Length Determination. These polymers were all synthesized by amine-initiated ring-opening polymerization of γ-benzyl-L-glutamate *N*-carboxyanhydride (Bz-glu-NCA) to yield poly(benzyl-L-glutamate) (PBLG), with the functional end group provided by the initiator. Furfurylamine was used as the initiator to synthesize the polymer backbone for the F-series polymers. 2,2-Dimethyl-1,3-dioxolane-4-methanamine was used as the initiator to synthesize PBLG for the P- and P-Py series of polymers (Scheme 1−3). In the reactions, the initial concentration of *N*-carboxyanhydride was ca. 14 wt %. These reactions were carried out at 0 °C for ca. 6 h. The number-average degrees of polymerization (DP_n) were determined by ^{1}H NMR by comparing the integrals of signals of the end-group protons (6.2−6.4 ppm for the furan end group for **F1** and 1.2−1.4 ppm for the acetonide-diol end group for **P1**) to those associated with the polymer pendant benzyl ester groups (6.8−7.2 ppm). Both polymers (**F1** and **P1**) were characterized by $DP_n \approx 30$, with an estimated error of ±5%. Nominal molecular weights (M_n^{GPC}) and polydispersites (PDI = M_w/M_n) of the polymers were measured by gel-permeation chromatography (GPC) in *N*-methyl-2-pyrrolidone (NMP) by reference to poly(methyl methacrylate) standards. In this way, we determined M_n^{GPC} = 4.6 kDa (PDI = 1.12) for **F1** and 4.9 kDa (1.06) for **P1**. The values of DP_n for both polymers were in good agreement with the [monomer]/[initiator] feed ratios.

The polymers were monitored by ^{1}H NMR and size-exclusion chromatography (SEC, GPC) after each pendant group transformation step, and they showed no significant changes in chain length. For the F-series of polymers, DP_n, determined by NMR, varied between 28 and 29 during the various pendant group transformation steps, whereas for the P-series of polymers, DP_n varied from 30 to 31. Nevertheless, we believe that the most accurate and precise values of DP_n were determined at the stage of PBLG. We therefore assume that these values remain unchanged as the polymer was taken through subsequent pendant group modification steps.

Postpolymerization Modification. For both the F- and P-series of polymers, the PBLG was treated with excess EDA to convert the benzyl ester to a polymer PGlu(EDA) with an -NH_2 on each repeat unit. This reaction employed conditions similar to those described previously in which PBLG was subjected to aminolysis with DET.[18,29,30] From the peak integration ratio of the methine protons adjacent to the amide on the polymer backbone (4.2−4.4 ppm) and the amide nitrogens of the pendant groups of PGlu(EDA) (2.8−3.6 ppm), we conclude that the conversion of PBLG to PGlu(EDA) was quantitative. ^{1}H NMR spectra of F-PGlu-(EDA) (**F2**) and P-PGlu(EDA) (**P2**) are presented in Figures S2 and S6, respectively, in the Supporting Information.

DTPA Coupling to F-Series Polymers. For the F-series polymer, the next step involved the attachment of DTPA units to each of the pendant amino groups. We followed a protocol that has been described previously[23] in which a large excess of DTPA (80 equiv relative to the amine groups on the polymer) was preactivated with a moderate excess of DMTMM (4 equiv relative to the amine groups on the polymer) as an amide coupling agent. By comparing the integrals of the ^{1}H NMR peaks at 2.8−3.6 ppm (the protons of the EDA pendant groups associated with the DTPAs) and the methine protons on the backbone (4.2−4.4 ppm), we showed that DTPA incorporation into the repeat units was quantitative.

Pendant Group Attachment to P- and P-Py-Series Polymers. In our design, approximately 10−15% of the pendant groups in these polymers would carry citraconimide (methylmaleimide, MMal) groups, to which NLS peptides

dx.doi.org/10.1021/bm500174p | *Biomacromolecules* 2014, 15, 2027−2037

would be attached. These peptides carried a terminal cysteine for Michael addition to the MMal groups. Although it is known that thiol addition to MMal is significantly slower (ca. 1000 times) than addition to maleimide itself,[31] MMal groups are hydrolytically more stable and show better stability than maleimides for long-term storage of thiol-reactive reagents.[32] Recall that the P-Py polymers differ from the P-polymers in that they also carry a small number of pyrene groups for UV detection of the polymer.

To begin, the pendant amines of P-PGlu(EDA) (**P2**) were treated with 6-citraconimido-hexanoic acid (CCHA) after preactivation with DMTMM. The number of MMal groups per polymer could be varied by adjusting the concentrations of DMTMM and CCHA. This reaction was followed by immediately adding DMTMM-activated DTPA into the reaction at pH 8.5. More specifically, for **P3**, we employed 2.4 equiv of DMTMM per polymer amine group, and for **P3Py**, we used 2.0 equiv of DMTMM. In these reactions, the mole ratio of DTPA to -NH_2 groups was ca. 80. The conditions used for adding DTPA to **P3Py** left some unreacted amine groups for later attachment of pyrene.

The fraction of the EDA pendant groups conjugated to MMal and DTPA was characterized by ^{1}H NMR, as shown in Figure 1. The number of MMal groups per polymer was calculated by comparing the integration of the signals of the maleimide proton (6.2−6.4 ppm) and the methine proton on the backbone (4.0−4.4 ppm), as described in the Supporting Information. The DTPA functionality on the polymer was calculated by comparing the sum of the integration of the signals in the ^{1}H NMR of DTPA and EDA (2.7−3.6 ppm) and integration of the signals of the backbone methine (4.2−4.4 ppm). For **P3**, MMal was present on ca. 13 ± 1% of the pendant groups, with DTPA on 81 ± 4% of the repeat units. We estimate the uncertainty in these values by assuming an error of ±5% in the integration of the DTPA signal and the MMal signal. We also found that DP_n remained equal to ca. 30, inferred by comparison of the integral of the acetonide-diol end group signal at 1.2−1.4 ppm to that of the methine backbone protons (4.2−4.4 ppm). Thus, for each **P3** polymer, there are, on average, 24 repeat units functionalized by DTPA, four functionalized by MMal, and approximately two unreacted amino groups. For **P3Py**, there are, on average, 22 DTPA units, five MMal groups, and three remaining amino groups per polymer.

End Group Modification. The polymers that we synthesized were designed to have a hydrazide end group that would form a covalent bond with aldehyde groups on the tmab−glycan generated by periodate oxidation. We use two distinct approaches to convert the chain ends of the F-series polymers and P-series polymers to hydrazide groups. Previous experiments in our laboratory demonstrated effective Diels−Alder coupling between furan-terminated DTPA polymers and a bismaleimide linker.[17] Thus, for the F-series polymers, we employed a Diels−Alder reaction between the maleimide group of EMCH and the furan on the polymer to introduce a hydrazide end group. Analysis of the product by ^{1}H NMR showed complete disappearance of the signals corresponding to the furfuryl end groups.

The P- and P-Py-series polymers were synthesized with an acetonide end group out of concern that a furan end group might not be compatible with MMal groups along the backbone. For these polymers, the acetonide protecting group was removed with a TFA/water (1:1 v/v) mixture. In ^{1}H NMR, the disappearance of the peaks for the acetonide-diol groups at 1.2−1.3 ppm implied the complete deprotection of the chain ends. It was at this stage that Py groups were introduced into the P-Py polymers by treating the polymer with an excess of 1-pyrenebutanoic acid succinimidyl ester (pyrene-NHS). Details are provided in the Supporting Information. After the reaction, this sample was first filtered through a syringe filter (PTFE, 0.2 μm) to remove the excess of pyrene derivatives and was then washed extensively with DI water and finally lyophilized to yield a white solid. Thermogravimetric analysis experiments on our previous DTPA-containing polymers prepared in this way showed that there were two Na^+ ions and two H_2O molecules associated with each DTPA.[16,18] Assuming a similar result here, we infer an effective molecular weight ($M_{n,eff}$) of 16 kDa for polymer **P6Py**. The pyrene content of **P6Py** was small, 0.22 pyrene per polymer (on average ca. one Py for every five polymer molecules). The Py content of the polymer was characterized by its UV−vis absorbance at 345 nm (Figure S15) by assuming an extinction coefficient ε = 33 500 $M^{-1}cm^{-1}$, which is the value determined for 1-pyrenebutyric acid in sodium carbonate buffer (pH 9.4, 200 mM, see the Supporting Information). The SEC trace (Figure S16) of the polymer in water monitored by both a refractive index detector and a UV−vis detector established that the pyrenes were covalently bound to the polymer.

To introduce hydrazide end groups, the polymers with the 1,2-diol-containing end groups were treated first with sodium periodate solution to generate an aldehyde end group and then with a mixture containing an excess of adipic acid dihydrazide (ADH, to form the hydrazone) and $NaBH_3CN$ to produce a stable linker. In more detail, the diol polymer (10 mg) was dissolved in phosphate buffer (2 mL, 100 mM, pH 6.0) in a brown glass vial to protect the solution from light. Then, sodium periodate solution (0.4 mL, 100 mM) was added, and the solution was incubated for 30 min at room temperature. Following washing with ammonium acetate buffer (3.0 mL, pH 4.5, 260 mM) in a spin filter, the sample was transferred to another vial. This solution in ammonium acetate buffer (3.0 mL, pH 4.5, 260 mM) was then treated with ADH (0.4 mmol) and a sodium cyanoborohydride solution (0.1 mL, 5 M in 1 M NaOH). The mixture was stirred for 5 h. After the solution was purified by spin filter (3.5 kDa MWCO), the sample was lyophilized to yield a white powder that was stored for future use. We refer to the hydrazine end-capped polymers generically as hy−MCP.

Unfortunately, the conversion of the end group of the polymer could not be determined by ^{1}H NMR: the end group signals of adipic acid dihydrazide overlapped with the peaks of the polymer. To test the effectiveness of the end group modification, we employed a model reaction using *t*-butyl carbazate to modify the polymer end. *t*-Butyl carbazate, a mono-*t*-Boc-protected hydrazine, has a ^{1}H NMR peak at ca. 1.3 ppm that does not overlap with any peaks of the polymer. In order to conserve valuable sample for cell studies, this model reaction was carried out on a different sample of **P4** that had an average of only one MMal per polymer. The reaction conditions followed those described in the previous paragraph (for details, see the Supporting Information). After the solution was purified using a spin filter, we compared the integration values of the *t*-Boc peak on the polymer end and the backbone methine protons. This experiment showed that end group conversion was nearly complete (ca. 97%, Figure S9). By assuming that the reactivities of the hydrazide groups on ADH

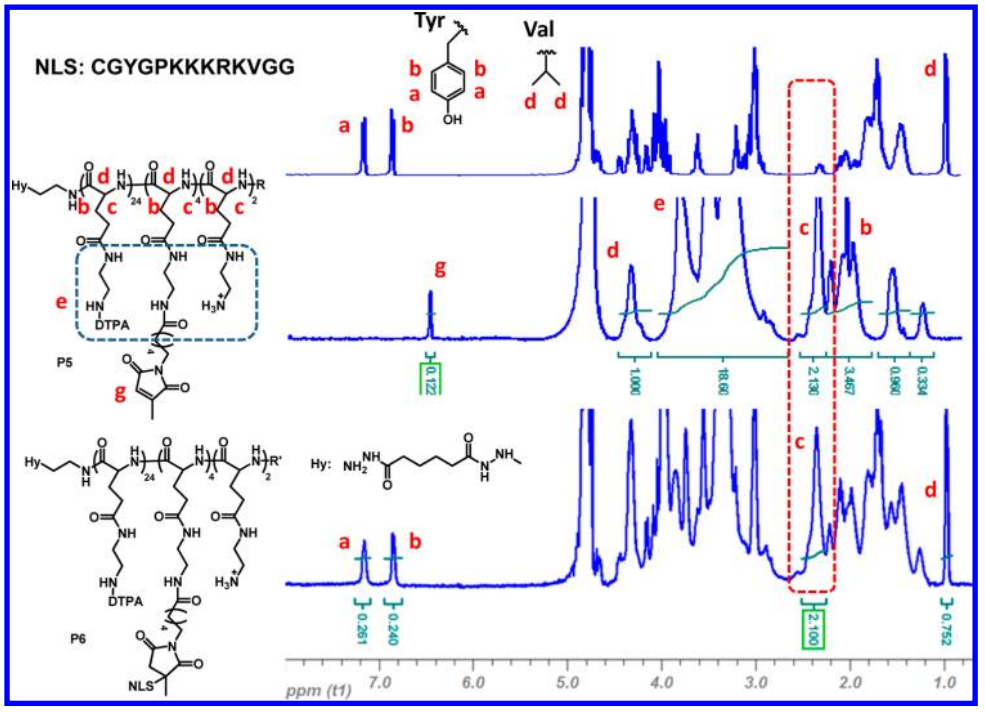

Figure 2. Determination of the number of NLS peptides by comparing the ^{1}H NMR spectra of the NLS peptide with the spectra of **P5** and **P6**. ^{1}H NMR analysis (comparison of the integration of the phenol protons on tyrosine, a and b, methyl protons on valine, d, and the protons on the polyglutamide backbone, c) shows the number of NLS peptides per polymer to be 3.8 on average, which is consistent with the number of citraconimide group per polymer (ca. 4). R and R′ are defined in Scheme 2 and in the caption to Figure 1.

Scheme 4. Synthesis and Radiolabeling of a Trastuzumab−Metal-Chelating Polymer Immunoconjugate (tmab−hy−MCP) or a Trasutuzmab−(*p*-NH$_2$-Bn-DTPA) Immunoconjugate (tmab−NH-Bn-DTPA)

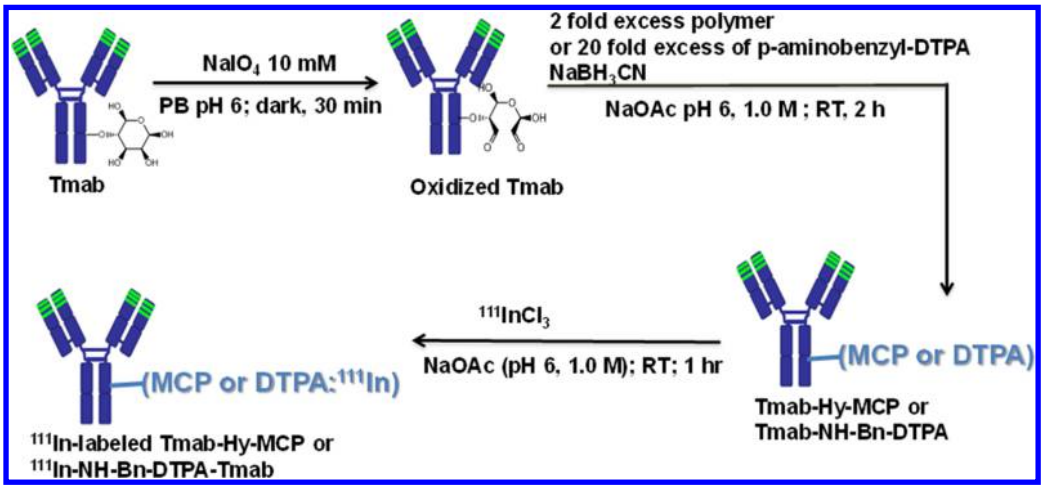

and *t*-butyl carbazate are similar, we infer nearly complete end group transformation in the synthesis of polymers **P6** and **P7Py**.

NLS Ligation. RICs based on tmab labeled with ^{111}In through DTPA and modified with 13-mer peptides (CGYGPKKKRKVGG) harboring the NLS from the simian virus 40 (SV40) large T-antigen have been reported recently.[4,5] These RICs exhibited enhanced nuclear uptake and cytotoxicity without loss of receptor-binding ability in vitro (SK-Br-3 and MDA-MB-361 cells) and without affecting tumor localization in immunocompromised mice compared to that of tmab alone or a RIC (^{111}In-trastuzumab) without NLS peptides. To test whether NLS peptides also enhance delivery of ^{111}In-labeled tmab−MCP conjugates to the nucleus for in vitro studies with SK-Br-3 cells, we designed the P- and P-Py-series polymers to carry multiple copies of the SV40 NLS at the periphery of the pendant groups.

The SV40 NLS ligation (addition of cysteine-SH to MMal groups) was carried out in HEPES buffer (pH 7.4, 0.5 M, 3 mL) for 2 h in the presence of 5 mM tris (2-carboxyethyl) phosphine hydrochloride (TCEP). Both of the NLS-containing polymers showed characteristic amino-acid peaks (Tyr δ, 6.6−7.2 ppm; Val δ, 0.7−0.9 ppm) in their respective ^{1}H NMR spectra (Figures 2, S10, and S13). Disappearance of the MMal signal at 6.2−6.4 ppm suggests complete conversion. Integration of peptide signals from Tyr and Val compared to the backbone signal (2.0−2.2 ppm, no NLS signal) indicated four peptides per polymer, which is consistent with the number

dx.doi.org/10.1021/bm500174p | *Biomacromolecules* 2014, 15, 2027−2037

of reactive citraconimide groups in their precursors (**P5** and **P6Py**). The UV spectrum of P7Py shows that it contains 0.23 pyrenes per polymer. This number also agrees with the precursor P6Py (0.22 per polymer).

Conjugation of hy−MCP to Trastuzumab and Radiolabeling with ^{111}In. The steps of glycan oxidation of tmab, conjugation with hy−MCP (tmab−hy−MCP) and radiolabeling with ^{111}In are outlined in Scheme 4. In parallel, we also prepared a tmab immunoconjugate with *p*-aminobenzyl-DTPA (tmab−NH-Bn-DTPA). Under the oxidation conditions we employed (molar ratio $NaIO_4$/tmab = 200:1, 23 °C, 30 min), we obtained 2.8 ± 1.7 aldehydes per tmab, as determined by the colorimetric Purpald assay.[27] Immediately afterward, the oxidized tmab was treated with a 2-fold molar excess of hy−MCP followed by addition of $NaBH_3CN$. To estimate the number of MCPs per tmab, we prepared a similar conjugate with a pyrene-labeled hydrazide−MCP (**P7Py**). The MCP content in the immunoconjugate was determined by comparing the absorbance of the solution at 345 nm (characteristic of pyrene) with that at 280 nm (tmab) after correcting the 280 nm absorbance for the contribution of MCP, with 0.23 pyrene on average. In this way, we found the number of **P7Py** per tmab was 1.4 ± 0.5.

The tmab−hy−MCP immunoconjugates were radiolabeled with ^{111}In as a solution of $^{111}InCl_3$ (3.7 MBq) in NaOAc buffer (1.0 M, pH 6.0). The labeling efficiency and radiochemical purity of the ^{111}In-labeled tmab−hy−MCP were >95% (n = 3), as determined by ITLC−SG. The conjugation of hy−MCP (**F4**) to tmab was examined by SE−HPLC after labeling with ^{111}In (Figure 3). The narrower peak (dark trace, Figure 3) was

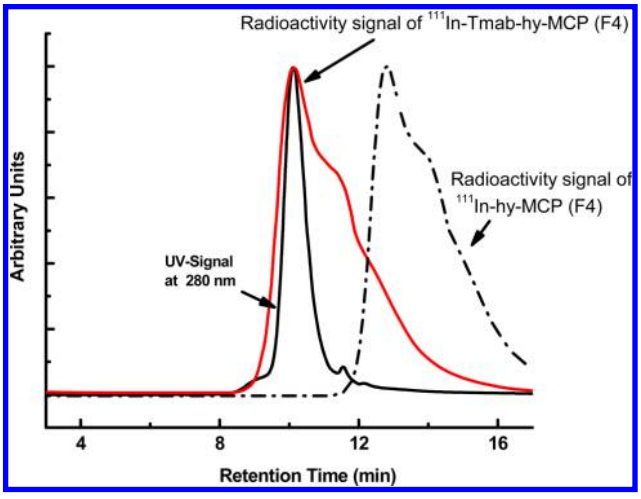

Figure 3. SE−HPLC chromatogram of tmab−hy−MCP (**F4**) and hy−MCP (**F4**) after radiolabeling with ^{111}In [flow rate, 0.35 mL/min; BioSep SEC-4000 SEC column; eluent, sodium phosphate buffer (100 mM, pH 7.0); UV detector, 280 nm; and a flow scintillation analyzer radioactivity detector]. The broader peak seen for the radioactivity signal compared to the UV signal for the tmab−polymer conjugate is a consequence of the larger volume of the detector channel for the radioactivity detector.

the response of the UV detector at 280 nm. The broader peak with the same peak maximum (red trace, Figure 3) is the signal from the radioactivity detector. The larger diameter of this flow cell leads to peak broadening. The overlay of the UV signal (280 nm), which detects tmab and the radioactivity signal that detects ^{111}In bound to the polymer, confirmed the formation of the RIC. We also used the radioactivity detector to examine the SE−HPLC chromatogram of the ^{111}In-labeled polymer itself, not conjugated to tmab. The signal resulting from ^{111}In−hy−MCP (**F4**) (dashed trace, Figure 3) appears at a much longer retention time than the ^{111}In-labeled tmab−hy−MCP (**F4**) immunoconjugate. The shift in the elution for ^{111}In−hy−MCP (**F4**) to a shorter retention time after conjugation to tmab is a consequence of the increase of the hydrodynamic volume of the MCP−tmab complex. This result also confirms that the polymer was conjugated to tmab.

A reviewer asked us to comment on the relative strength of binding of trivalent metal ions to the DTPA monoamide pendant groups of the metal-chelating polymers compared to the binding to DTPA itself. The preferred coordination number of In^{3+} is six, but the DTPA−In^{3+} complex has a coordination number of eight.[33,34] For many years, authors assumed that the In^{3+} complex with DTPA monoamide (DTPA-Am) was seven coordinate,[33,35] but a crystal structure of the In^{3+} complex with DTPA-diamide showed that this complex also was octadentate, with the amide carbonyls of DTPA diamide serving the function of the carboxylates of DTPA itself.[36] We depict the octadentate complex of In^{3+} with the DTPA-Am on the pendant group of our polymer in Figure 4.

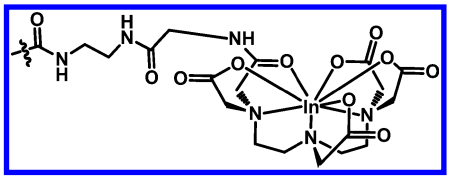

Figure 4. Octadentate complex of In^{3+} with DTPA-monoamide pendant group of a MCP. The complex has a net charge of −1.

The issue of how conversion of one of the carboxylates of DTPA to an amide affects the dissociation constant of the complex was addressed initially by Sherry and co-workers for complexes with Gd^{3+}.[37] They measured the binding of Gd^{3+} ions to DTPA and DTPA-monoamide (DTPA-Am). Both ligands form octadentate complexes. Although the thermodynamic binding constant for DTPA ($DTPA^{5-} + Gd^{3+} \rightarrow$ DTPA-Gd^{2-}) is about 4 orders of magnitude stronger than that of DTPA-Am (DTPA-$Am^{4-} + Gd^{3+} \rightarrow$ DTPA-Am-Gd^{-}), the important value to be considered is the difference in the conditional dissociation constants that operate at a given pH. Amidation of one of the carboxylates of DTPA changes its pK_a values so that, at pH 7.4 in the presence of 0.1 M NaCl, the value for DTPA-Am-Gd^{-} is only log K = 1.2 different than that for DTPA-Gd^{2-}, and at pH 6, the two values are essentially identical. There is, in addition, a more subtle feature of the metal binding associated with the multiple chelators in the MCP. Isothermal titration calorimetry studies of Gd^{3+} binding at pH 5.5 to an MCP with multiple (50) DTPA-monoamide pendant groups showed that the proximity of multiple DTPA groups led to stronger binding of metal ions at the beginning of the titration and weaker binding when the polymer approached saturation.[24] It is possible to infer from these data that at pH 6.0, where the MCPs in this study were loaded with traces of $^{111}In^{3+}$, the metal ions bind more strongly to the DTPA-monoamide pendant groups of the polymer than to DTPA itself.

HER2 Immunoreactivity. To assess antigen recognition of the ^{111}In-labeled tmab−hy−MCP conjugates, the specific

binding to SK-Br-3 cells (1.3×10^6 HER2 receptors/cell) was examined in direct binding assays in the absence and the presence of excess tmab.[12] The extent of specific binding was compared to that of ^{111}In−NH-Bn-DTPA−tmab. The fraction of specific binding is defined as the fraction of binding that can be blocked (i.e., competed out) by excess unlabeled tmab to HER2 sites on the cell surface.

The results of these assays are shown in Figure 5 and are presented as the percentage of RICs bound to 1×10^6 SK-Br-3

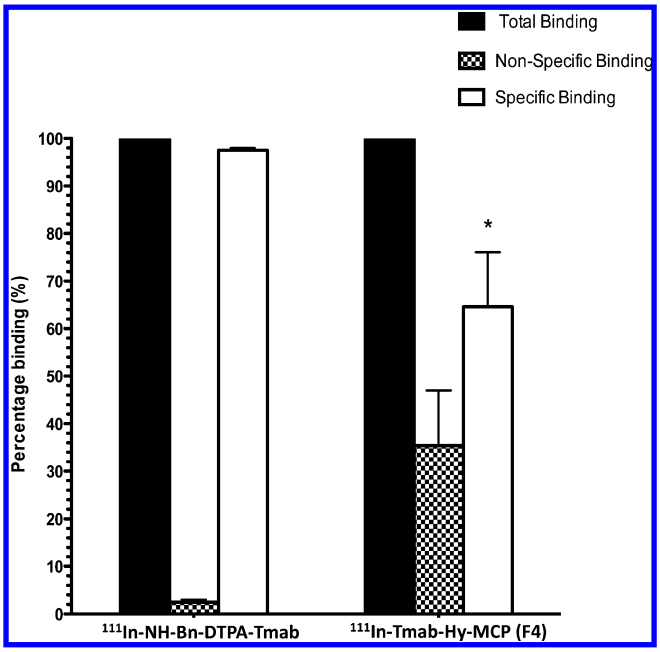

Figure 5. Percent binding of ^{111}In-labeled RICs to HER2$^+$ SK-Br-3 BC cells. Values are shown as the mean ± SD (n = 3). * Significant differences ($p < 0.05$) between specific binding of the two ^{111}In-RICs.

cells. For ^{111}In−NH-Bn-DTPA−tmab, the proportion of specific binding was very high, 97.5 ± 0.5%. In contrast, the proportion of specific binding for ^{111}In-labeled tmab−hy−MCP (**F4**) conjugation was significantly lower, 64.5 ± 11.5% ($p < 0.05$). We obtained two important results from this assay. First, we learned that although HER2 receptor binding was reduced relative to ^{111}In−NH-Bn-DTPA−tmab under the same conditions there was, nevertheless, preserved specific binding to HER2; thus, Fc-directed substitution of one or two polymer molecules per tmab was feasible. In addition, we learned that the presence of the MCP promotes binding to the cells, which is not related to HER2 because it could not be blocked with an excess of tmab. Although the origin of this nonspecific binding in not known, it may be associated with electrostatic effects associated with the negative charges along the polymer backbone. This is a potential consideration that may impact the therapeutic use of these RICs, although the extent of nonspecific binding mediated by the polymers to tissues remains to be evaluated.

To investigate the effect of polymer conjugation on HER2 immunoreactivity further, indirect competition−receptor binding assays were conducted using SK-Br-3 cells, where ^{111}In−NH-Bn-DTPA−tmab (K_D = 3.2 nM; Figure S18) was displaced by increasing concentrations of unlabeled tmab−hy−MCPs (**F4** or **P6**). As shown in Figure 6, HER2 specific binding of ^{111}In−NH-Bn-DTPA−tmab to SK-Br-3 cells was displaced by unlabeled tmab−hy−MCP (**F4** or **P6**). The EC_{50} values for

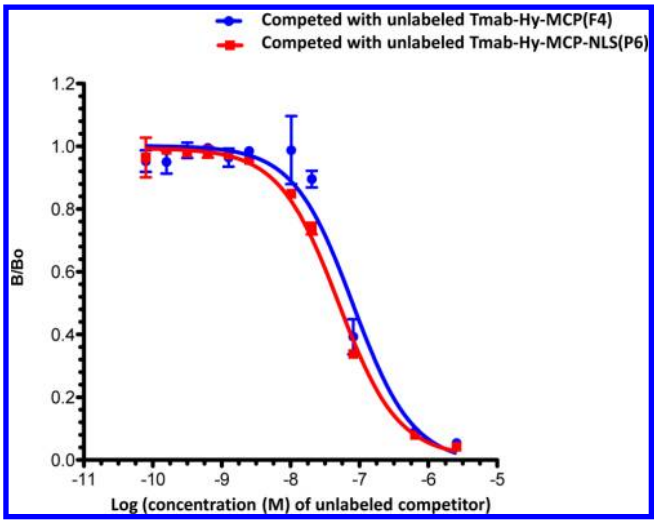

Figure 6. Competition binding curve showing the displacement of the binding of ^{111}In−NH-Bn-DTPA−tmab (20 nM; K_D = 3.2 nM) in the presence of increasing concentrations (0−2600 nM) of unlabeled tmab−hy−MCP (**F4**) or unlabeled tmab−hy−MCP−NLS (**P6**) to HER2$^+$ SK-Br-3 breast cancer cells. B = radioligand bound in the presence of competitor. B_o = radioligand bound in the absence of competitor. Values shown are the mean ± SD (n = 3). EC_{50} values are 71.8 ± 11.1 and 49.6 ± 3.4 nM for tmab−hy−MCP (**F4**) and tmab−hy−MCP−NLS (**P6**), respectively ($p < 0.05$). The calculated dissociation constants, K_D, are 10.0 ± 1.5 for tmab−hy−MCP (**F4**) and 6.9 ± 0.5 nM for tmab−hy−MCP−NLS (**P6**) ($p < 0.05$).

displacement of ^{111}In−NH-Bn-DTPA−tmab were 71.8 ± 11.1 nM for tmab−hy−MCP (**F4**) and 49.6 ± 3.4 nM for tmab−hy−MCP−NLS (**P6**). The dissociation constants, K_D, calculated from these experiments were 10.0 ± 1.5 nM for tmab−hy−MCP (**F4**) and 6.9 ± 0.5 nM for tmab−hy−MCP−NLS (**P6**), as determined from data fitted to a one-site competition binding model. Although the displacement concentrations for **F4** and **P6**, and the corresponding K_D values, differed by less than a factor of 2, they were significantly different ($p < 0.05$). These K_D values are comparable to the K_D values for ^{111}In−NH-Bn-DTPA−tmab (K_D = 3.2 ± 1.2 nM, shown in Figure S18) and ^{111}In−tmab (tmab derivatized with DTPA dianhydride and labeled with ^{111}In, K_D = 8.2 ± 0.5 nM) binding to SK-Br-3 cells.[2] The competition−receptor binding assays demonstrated that neither the MCPs nor the presence of the NLS peptides had a major effect on the ability of tmab to displace the binding of ^{111}In−NH-Bn-DTPA−tmab to HER2.

CONCLUSIONS

We synthesized three types of well-defined polyglutamide-based metal-chelating polymers, each with a hydrazide end group and a number-average degree of polymerization of 30. The F-series polymers were synthesized with a furan end group. Each of the pendant groups carried DTPA as a metal-chelating moiety. For this polymer, the hydrazide end was introduced via a Diels−Alder reaction between the furan and EMCH. The P-series of metal-chelating polymers was designed to carry several copies (ca. four) of a NLS peptide along the backbone in addition to the DTPA metal-chelating groups. Here, the hydrazide was introduced by a reaction of adipic acid dihydrazide with an aldehyde generated on one end of the polymer. The P-Py series of polymers was similar to the P-series but also included a small number of pyrene chromophores (less than one per chain) along the backbone

to allow for UV detection of the metal-chelating polymer. In this way, we were able to employ a spectrophotometric assay to estimate the mean number of MCPs per tmab. These hydrazide-terminated polymers were site-specifically conjugated to aldehyde groups generated by $NaIO_4$ oxidation of the pendant glycan in the Fc domain of tmab. The resulting immunoconjugates were radiolabeled with ^{111}In and examined by SE−HPLC to confirm the attachment of the polymer to the antibody.

Immunoreactivity assays demonstrated, first, that neither the MCPs nor the presence of the NLS peptides interfered with recognition of the RICs of HER2 expressed on SK-Br-3 cells, although nonspecific binding was increased with polymer conjugation. Second, displacement experiments showed that these MCPs had no significant effect on the binding affinity between the tmFab and HER2 receptors, with K_D values in the low nanomolar range for each polymer.

The main purpose of this study was to report the synthesis of the three classes of metal-chelating polymers, their conjugation to tmab, and the labeling and immunoreactivity of the resulting radioimmunoconjugates. In ongoing experiments, we are examining the internalization of these immunoconjugates by SK-Br-3 cells and the role of the NLS peptides on nuclear localization. These results will be the subject of a future publication.

■ ASSOCIATED CONTENT

Supporting Information

Experimental details for the syntheses of citraconimidohexanoic acid (CCHA) and all polymers (**F1−F4**, **P1−P6**, and **P3Py−P7Py**), representative ^{1}H NMR spectra of these compounds, UV−vis spectra and calibration curve of 1-pyrenebutyric acid solution, UV−vis spectra of **P6Py** and **P7Py** at a concentration of 1.8 mg/mL, SEC profiles of **P6Py** with a UV detector and a refractive index detector, and direct (saturation) binding of ^{111}In-NH-Bn-DTPA-Tmab to HER2$^+$ SK-Br-3 human breast cancer cells in the absence or presence of a 50-fold excess of unlabeled tmab. This material is available free of charge via the Internet at http://pubs.acs.org.

■ AUTHOR INFORMATION

Corresponding Authors

*(R.M.R.) E-mail: raymond.reilly@utoronto.ca.

*(M.A.W.) E-mail: mwinnik@chem.utoronto.ca.

Author Contributions

⊥These authors contributed equally to this work.

Notes

The authors declare no competing financial interest.

■ ACKNOWLEDGMENTS

We acknowledge financial support from the Canadian Institutes of Health Research/Natural Sciences and Engineering Research Council Collaborative Health Research Program (grant no. CHRPJ 365423-09; CPG-95268) and from DVS Sciences, Inc. We also thank Isaac Herrera for his valuable comments and discussion.

■ REFERENCES

(1) McKeage, K.; Perry, C. M. *Drugs* **2002**, *62*, 209−243.

(2) Mitri, Z.; Constantine, T.; O'Regan, R. *Chemother. Res. Pract.* **2012**, *2012*, 743193-1−743193-7.

(3) Hudis, C. A. *N. Engl. J. Med.* **2007**, *357*, 39−51.

(4) Costantini, D. L.; Chan, C.; Cai, Z.; Vallis, K. A.; Reilly, R. M. *J. Nucl. Med.* **2007**, *48*, 1357−1368.

(5) Costantini, D. L.; Hu, M.; Reilly, R. M. *Cancer Biother. Radiopharm.* **2008**, *23*, 3−24.

(6) Rosenblum, M. G.; Horn, S. A.; Cheung, L. H. *Int. J. Cancer* **2000**, *88*, 267−273.

(7) Batra, J. K.; Kasprzyk, P. G.; Bird, R. E.; Pastan, I.; King, C. R. *Proc. Natl. Acad. Sci. U.S.A.* **1992**, *89*, 5867−5871.

(8) Coyne, C. P.; Ross, M. K.; Bailey, J. G. *J. Drug Targeting* **2009**, *17*, 474−489.

(9) Lambert, J. M. *Curr. Opin. Pharmacol.* **2005**, *5*, 543−549.

(10) Dugger, D. L.; Sliwkowski, M. X.; Spencer, S. D.; Kenkare-Mitra, S. R.; Phillips, G. D. L.; Li, G.; Schwall, R. H.; Crocker, L. M.; Parsons, K. L.; Mai, E.; Blättler, W. A.; Lambert, J. M.; Chari, R. V. J.; Lutz, R. J.; Wong, W. L. T.; Jacobson, F. S.; Koeppen, H. *Cancer Res.* **2008**, *68*, 9280−9290.

(11) Ducry, L.; Stump, B. *Bioconjugate Chem.* **2010**, *21*, 5−13.

(12) Costantini, D. L.; Bateman, K.; McLarty, K.; Vallis, K. A.; Reilly, R. M. *J. Nucl. Med.* **2008**, *49*, 1498−1505.

(13) Wadas, T. J.; Wong, E. H.; Weisman, G. R.; Anderson, C. J. *Chem. Rev.* **2010**, *110*, 2858−2902.

(14) Wong, J. Y. C.; Raubitschek, A.; Yamauchi, D.; Williams, L. E.; Wu, A. M.; Yazaki, P.; Shively, J. E.; Colcher, D.; Somlo, G. *Cancer Biother. Radiopharm.* **2010**, *25*, 387−394.

(15) Perik, P. J.; Lub-De Hooge, M. N.; Gietema, J. A.; van der Graaf, W. T. A.; de Korte, M. A.; Jonkman, S.; Kosterink, J. G. W.; van Veldhuisen, D. J.; Sleijfer, D. T.; Jager, P. L.; de Vries, E. G. E. *J. Clin. Oncol.* **2006**, *24*, 2276−2282.

(16) Liu, P.; Boyle, A. J.; Lu, Y.; Reilly, R. M.; Winnik, M. A. *Biomacromolecules* **2012**, *13*, 2831−2842.

(17) Boyle, A. J.; Liu, P.; Lu, Y.; Weinrich, D.; Scollard, D. A.; Ngo Njock Mbong, G.; Winnik, M. A.; Reilly, R. M. *Pharm. Res.* **2013**, *30*, 104−116.

(18) Lu, Y.; Chau, M.; Boyle, A. J.; Liu, P.; Niehoff, A.; Weinrich, D.; Reilly, R. M.; Winnik, M. A. *Biomacromolecules* **2012**, *13*, 1296−1306.

(19) Patil, V.; Gada, K.; Panwar, R.; Varvarigou, A.; Majewski, S.; Weisenberger, A.; Ferris, C.; Tekabe, Y.; Khaw, B.-A. *Eur. J. Nucl. Med. Mol. Imaging* **2012**, *39*, 824−839.

(20) Liu, P.; Cai, Z.; Kang, J. W.; Boyle, A. J.; Adams, J.; Lu, Y.; Ngo Ndjock Mbong, G.; Sidhu, S.; Reilly, R. M.; Winnik, M. A. *Biomacromolecules* **2014**, *15*, 715−725.

(21) Schechter, B.; Arnon, R.; Colas, C.; Burakova, T.; Wilchek, M. *Kidney Int.* **1995**, *47*, 1327−1335.

(22) Lou, X.; Zhang, G.; Herrera, I.; Kinach, R.; Ornatsky, O.; Baranov, V.; Nitz, M.; Winnik, M. A. *Angew. Chem.* **2007**, *119*, 6223−6226.

(23) Majonis, D.; Herrera, I.; Ornatsky, O.; Schulze, M.; Lou, X.; Soleimani, M.; Nitz, M.; Winnik, M. A. *Anal. Chem.* **2010**, *82*, 8961−8969.

(24) Illy, N.; Majonis, D.; Herrera, I.; Ornatsky, O.; Winnik, M. A. *Biomacromolecules* **2012**, *13*, 2359−2369.

(25) Rodwell, J. D.; Alvarez, V. L.; Lee, C.; Lopes, A. D.; Goers, J. W.; King, H. D.; Powsner, H. J.; McKearn, T. J. *Proc. Natl. Acad. Sci. U.S.A.* **1986**, *83*, 2632−2636.

(26) Fuller, W. D.; Verlander, M. S.; Goodman, M. *Biopolymers* **1976**, *15*, 1869−1871.

(27) Quesenberry, M. S.; Lee, Y. C. *Anal. Biochem.* **1996**, *234*, 50−55.

(28) McLarty, K.; Cornelissen, B.; Scollard, D. A.; Done, S. J.; Chun, K.; Reilly, R. M. *Eur. J. Nucl. Med. Mol. Imaging* **2009**, *36*, 81−93.

(29) De Marre, A.; Soyez, H.; Schacht, E.; Pytela, J. *Polymer* **1994**, *35*, 2443−2446.

(30) Itaka, K.; Ishii, T.; Hasegawa, Y.; Kataoka, K. *Biomaterials* **2010**, *31*, 3707−3714.

(31) Guy, J.; Castonguay, R.; Campos-Reales Pineda, N. B.; Jacquier, V.; Caron, K.; Michnick, S. W.; Keillor, J. W. *Mol. BioSyst.* **2010**, *6*, 976−987.

(32) Hong, L. P. T.; Scoble, J. A.; Doughty, L.; Coia, G.; Williams, C. C. *Aust. J. Chem.* **2011**, *64*, 779−789.

(33) Maecke, H. R.; Riesen, A.; Ritter, W. *J. Nucl. Med.* **1989**, *30*, 1235−1239.
(34) Palenik, G. J.; Dymock, K. R. *Acta Crystallogr., Sect. B* **1980**, *36*, 2059−2063.
(35) Arano, Y.; Uezono, T.; Akizawa, H.; Ono, M.; Wakisaka, K.; Nakayama, M.; Sakahara, H.; Konishi, J.; Yokoyama, A. *J. Med. Chem.* **1996**, *39*, 3451−3460.
(36) Hsieh, W.-Y.; Liu, S. *Inorg. Chem.* **2004**, *43*, 6006−6014.
(37) Sherry, A. D.; Cacheris, W. P.; Kuan, K.-T. *Magn. Reson. Med.* **1988**, *8*, 180−190.